RESEARCH ARTICLE OPEN ACCESS

# Effects of a Small-Molecule Perforin Inhibitor in a Mouse Model of CD8 T Cell–Mediated Neuroinflammation

Carmen Gonzalez-Fierro, MSc, Coralie Fonte, PhD, Eloïse Dufourd, MSc, Vincent Cazaentre, BSc, Sidar Aydin, PhD, Britta Engelhardt, PhD, Rachel R. Caspi, PhD, Biying Xu, PhD, Guillaume Martin-Blondel, MD, PhD, Julie A. Spicer, PhD, Joseph A. Trapani, MD, PhD, Jan Bauer, PhD, Roland S. Liblau, MD, PhD, and Chloé Bost, PharmD, PhD

**Correspondence**
Dr. Liblau
roland.liblau@inserm.fr

*Neurol Neuroimmunol Neuroinflamm* 2023;10:e200117. doi:10.1212/NXI.0000000000200117

## Abstract

### Background and Objectives

Alteration of the blood-brain barrier (BBB) at the interface between blood and CNS parenchyma is prominent in most neuroinflammatory diseases. In several neurologic diseases, including cerebral malaria and Susac syndrome, a CD8 T cell–mediated targeting of endothelial cells of the BBB (BBB-ECs) has been implicated in pathogenesis.

### Methods

In this study, we used an experimental mouse model to evaluate the ability of a small-molecule perforin inhibitor to prevent neuroinflammation resulting from cytotoxic CD8 T cell–mediated damage of BBB-ECs.

### Results

Using an in vitro coculture system, we first identified perforin as an essential molecule for killing of BBB-ECs by CD8 T cells. We then found that short-term pharmacologic inhibition of perforin commencing after disease onset restored motor function and inhibited the neuropathology. Perforin inhibition resulted in preserved BBB-EC viability, maintenance of the BBB, and reduced CD8 T-cell accumulation in the brain and retina.

### Discussion

Therefore, perforin-dependent cytotoxicity plays a key role in the death of BBB-ECs inflicted by autoreactive CD8 T cells in a preclinical model and potentially represents a therapeutic target for CD8 T cell–mediated neuroinflammatory diseases, such as cerebral malaria and Susac syndrome.



From the Toulouse Institute for Infectious and Inflammatory Diseases (Infinity) (C.G.-F., C.F., E.D., V.C., G.M.-B., R.S.L., C.B.), University of Toulouse, CNRS, INSERM, UPS, France; Theodor Kocher Institute (S.A., B.E.), University of Bern, Switzerland; Laboratory of Immunology (R.R.C., B.X.), National Eye Institute, National Institutes of Health, Bethesda, MD; Department of Infectious and Tropical Diseases (G.M.-B.), Toulouse University Hospital, France; Auckland Cancer Society Research Centre (J.A.S.), Faculty of Medical and Health Sciences, The University of Auckland, New Zealand; Cancer Immunology Program (J.A.T.), Peter MacCallum Cancer Centre, Melbourne, Australia; Sir Peter MacCallum Department of Oncology (J.A.T.), The University of Melbourne, Parkville, Australia; Department of Neuroimmunology (J.B.), Center for Brain Research, Medical University of Vienna, Austria; and Department of Immunology (R.S.L., C.B.), Toulouse University Hospital, France.

Go to Neurology.org/NN for full disclosures. Funding information is provided at the end of the article.

The Article Processing Charge was funded by INSERM.

## Glossary

**APC** = antigen-presenting cell; **BBB** = blood-brain barrier; **CTLs** = cytotoxic CD8 T cells; **EC** = endothelial cell; **ECM** = experimental cerebral malaria.

Most diseases of the CNS involve the local recruitment and/or activation of cells of the innate and adaptive immune system.[1] In a large number of neurologic diseases, recruitment and persistence of T cells in the CNS parenchyma likely contribute to the pathogenic process. Indeed, such T-cell infiltration has been shown in infectious diseases,[2] autoimmune diseases,[3,4] vascular diseases of the CNS,[5] and even neurodegenerative diseases.[6,7] Intriguingly, in these situations, CD8 T cells dominate, sometimes by a large extent, over the CD4 T-cell compartment. For instance, in MS, a very clear preponderance of CD8 over CD4 T cells is observed in perivascular cuffs and parenchymal lesions from biopsies or postmortem tissue,[8] and concordant studies revealed the oligoclonal feature of CD8 T cells isolated from the cerebral parenchyma or CSF.[9,10]

In some inflammatory/autoimmune diseases of the CNS, data even suggest that CD8 T cell–mediated cytotoxicity directly contributes to tissue damage. For instance, in paraneoplastic neurologic syndromes with autoimmunity against the intracellular Hu or Yo proteins, the brain parenchymal inflammatory infiltrates are mainly composed of CD8 T cells, which form aggregates located near neurons.[11-13] Moreover, in MS and related syndromes, a large fraction of tissue-resident CD8 T cells express granzyme B.[4,14]

Transmigration of immune cells from the blood circulation across the blood-brain barrier (BBB) into the CNS is a critical event for the development of autoimmune neuroinflammation. The endothelial cells (ECs) of the BBB serve as an important partner in the multistep process of immune cell transmigration, involving adhesion and signaling molecules (e.g., VCAM-1 and ICAM-1).[15] The diapedesis process and its associated proteins have been shown to be upregulated under inflammatory conditions[16] and can occur independently of antigen recognition.[17,18] Apart from diapedesis, damage to BBB-ECs may also enable pathogenic T cells to migrate into the brain parenchyma. ECs express MHC class I[19] and costimulatory molecules[20] and can be induced to secrete cytokines and chemokines, some of which are chemoattractant for activated CD8 T cells.[21-24] In principle, ECs may therefore act as unconventional antigen-presenting cells (APCs) that might facilitate antigen-specific CD8 T-cell infiltration in brain tissue.[25] BBB disruption by antigen-specific cytotoxic CD8 T cells would thus set up a "vicious cycle" of local inflammation leading to T-cell penetration into brain tissue and then progressively greater inflammation and amplified T-cell accumulation.

In this study, we examined the ability of a highly focused immunosuppressive agent that specifically blocks the function of perforin[26,27] to prevent CD8 T cell–induced neuroinflammation by maintaining the integrity of the EC barrier when ECs are themselves targeted by autoreactive CD8 T cells. This mechanism underlies the pathogenesis of cerebral malaria and a rare human autoimmune disorder, Susac syndrome (SuS).[14,19,28]

Perforin, a calcium-dependent pore-forming protein, is the master regulator of the apoptosis pathways activated after the exocytosis of the cytotoxic granule contents of CD8 T cells because it is indispensable for proapoptotic serine proteases (granzymes) released with it to transit into the cytosol of the target cells, where they trigger cell death signaling.[29,30] We found that temporary pharmacologic inhibition of perforin markedly reduced the clinical signs in a mouse model of SuS, accompanied by preserved EC viability, maintenance of the BBB, and marked reduction in CD8 T-cell penetration into the brain and retina.

## Methods

### Mice

The so-called EC-HA$^+$ double-transgenic mice express the H1N1 *influenza* virus hemagglutinin (HA) in ECs from CNS microvessels, but not in other ECs. EC-HA$^+$ mice were generated by crossing the Rosa26-HA knock-in mice[31] with Slco1c1-CreERT2 mice.[32] The Slco1c1 promoter is active in ECs from the BBB but not in other types of ECs,[24] and Slco1c1-CreERT2 mice allow restricted expression in BBB-ECs in a tamoxifen-inducible manner.[14] However, Cre-mediated recombination also occurs in epithelial cells of the choroid plexus and a small number of cortical astrocytes and some hippocampal neurons. EC-HA$^+$ mice, and control littermate mice, referred to as EC-HA$^-$, were treated with intraperitoneal (i.p.) injections of tamoxifen (1 mg/mouse/d) for 5 consecutive days. Both female and male mice were used for experiments between the ages of 7 and 13 weeks. CL4-TCR transgenic mice expressing the CD45.1 congenic marker, source of the HA-specific CD8 T cells, have been previously described.[31] OT-I-TCR transgenic mice expressing the CD45.1 congenic markers that were the source of the ovalbumin-specific OT-I CD8 T cells have also been previously described.[33] All mice were bred on a [BALB/c x C57Bl/6]F1 background. Mice were kept in specific pathogen-free conditions in enriched cages of 5 companions maximum and in a light/dark controlled cycle.

### Preparation of Primary Cultures of HA-specific Cytotoxic CD8 T Cells (CTLs)

Lymph nodes and spleen of CD45.1$^+$ CL4-TCR mice were dilacerated, and erythrocytes were lysed using ammonium-chloride-potassium lysis buffer. CD8 T cells were then

purified by negative selection using DYNAL Dynabeads (ThermoFisher). To generate HA-specific CTLs, CD8 T cells were cocultured with irradiated (25 Gy) splenocytes at a 1:5 ratio, in the presence of 1 μg/mL $HA_{512-520}$ peptide (IYSTVASSL; Genecust), in DMEM supplemented with 10% FBS, 1% HEPES, 1% penicillin/streptomycin, and 0.1% 2-mercaptoethanol containing IL-2 (1 ng/mL, R&D systems) and IL-12 (20 ng/mL, R&D systems). IL-2 was further added on days 2 and 4. On day 5, HA-specific CTLs were collected by Ficoll density separation and used in in vitro and in vivo experiments. The CTL suspensions routinely contained >95% of $CD8^+V\beta8^+$ cells, and >70% were IFN-γ/TNF producers, as assessed by flow cytometry.

## Primary Mouse Brain Microvascular Endothelial Cell Culture

Cortices from double-transgenic EC-$HA^+$ and EC-$HA^-$ control mice were isolated by removing meninges, cerebellum, striatum, optic nerves, and brain white matter. Preparations were pooled and ground using a Dounce homogenizer in washing buffer, and then an enzymatic digestion and size selection by filtration were performed, as previously described.[34] Primary brain microvascular endothelial cells (BBB-ECs) obtained were seeded onto IBIDI-treated plaques (Ibidi) in DMEM with 20% FBS, 2% sodium pyruvate, 2% nonessential amino acids, 50 μg/mL of gentamycin, supplemented with 1 ng/mL of fibroblast growth factor, and 4 μg/mL of puromycin. After 48 hours, cells were cultured in medium supplemented only with 1 ng/mL of fibroblast growth factor until a confluent BBB-EC monolayer was obtained, usually at day 7 after plating.

## In Vitro Live Cell Imaging

In vitro live cell imaging was performed as described earlier.[35,36] CTL interactions with BBB-ECs in the flow chamber was allowed at a low shear (0.1 dyn/$cm^2$) for 5 minutes, followed by physiologic shear (1.5 dyn/$cm^2$) for an additional 20 minutes to assess the postarrest behavior. Images were acquired at 10x magnification with an inverted microscope (AxioObserver, Carl Zeiss) with phase-contrast and fluorescence illumination, every 10 seconds. Image analysis was performed using the ImageJ software. Thirty seconds after the onset of the enhanced shear, the numbers of arrested T cells were counted manually by using ImageJ. The postarrest behavior of T cells was defined as follows: T cells that actively sent protrusions underneath the ECs in a stationary position (probing); polarized T cells that continuously crawled on the ECs (crawling).

## Coculture of BBB-ECs Expressing HA or Not With HA-Specific CTLs

CTLs stained with cell trace violet (CTV; Thermofisher) were cocultured (8,000/well) onto the BBB-EC monolayer for 24 hours in DMEM supplemented with 20% FBS, 2% sodium pyruvate, 2% nonessential amino acids, and 50 μg/mL of gentamycin.

Expression of the activated form of caspase-3 by BBB-ECs was monitored using NucView 488 assay labeling (1 μL/mL, Biotium), a cell-permeant substrate, which on cleavage releases a high-affinity DNA fluorescent dye. Where indicated, the medium was supplemented with a small-molecule perforin inhibitor, SN34960, at 50 μM,[26,27,37] anti-mouse FasL antibody (20 μM, MFL3, Biolegend), both, or the perforin inhibitor diluent (DMSO) as control. Expression of activated caspase-3 by BBB-ECs was assessed using a Spinning disk/TIRF microscope (Roper, CSU X1) with an image (3 areas per well) taken every hour for 24 hours. The images were then analyzed using ImageJ, the CTV-stained CTLs being eliminated from the analysis. To quantify killing of BBB-ECs, the fixed BBB-ECs (70% methanol for 10 minutes) were incubated with rat antimouse claudin-5 monoclonal antibody (1/200, 4C3C2, Invitrogen) and then with Alexa488-labeled secondary goat antirat antibody (1/1,000, Life Technologies), 1 hour at room temperature each. Nuclei were stained with DAPI (1/1,000, BD). Immunofluorescence staining was assessed using the Apotome ZEISS microscope, and images (4 areas per well) were analyzed using ImageJ. The number of cells was counted using the DAPI staining.

## In Vivo Transfer of HA-Specific CTLs and Treatment With a Perforin Inhibitor

HA-specific CTLs or ovalbumin-specific OT-I CTLs expressing the CD45.1 marker ($10^6$ cells) were adoptively transferred i.v. to $CD45.2^+$ EC-$HA^+$ mice and EC-$HA^-$ littermate controls.[14] Motor skills and coordination were assessed daily using a Rotarod device (Bioseb) with acceleration from 4 to 40 rpm over a 600-second period. For training, mice were tested on 4 consecutive days. During the investigation period, the latency to fall was measured for each mouse just before CTL transfer (at D0) and then daily. The D0 value represents the 100% latency to fall.

For in vivo dosing, lyophilized perforin inhibitor SN34960 was dissolved in 20% (wt/vol) β-cyclodextrin or DMSO and injected i.p. (100 mg/kg in 200 μL) every 12 hours for 4 days.[26] This dosage was determined given the pharmacokinetics (elimination half-life of approximately 3 hours) and pharmacodynamics of compound SN34960.[38] The perforin inhibitor was prepared immediately before injection.

## Immunohistochemical Evaluation and Quantification of Mouse Tissues

At the indicated time points, mice received a lethal dose of ketamine and xylazine, and, after PBS perfusion, their brains were fixed in 10% PFA at 4°C for 24 hours and transferred into 70% ethanol. The fixed brains were dehydrated in ethanol and xylene baths and subsequently embedded in paraffin blocks. The light microscopical stainings were performed as previously described in detail.[39] The primary antibodies used were as follows: anti-CD3 (MA1-90582, Thermo Scientific), anti-CD31 (ab28364, Abcam), and biotinylated donkey-antimouse immunoglobulin (715-065-150, Jackson).

All secondary antibodies were purchased from Jackson. Streptavidin-HRP (Sigma) was used as third step. Quantification of $CD3^+$ T cells was performed by manual counting of stained cells in cerebellar tissue 4 $mm^2$ or by using a morphometric grid. The nucleus of approximately 250 $CD31^+$ ECs was examined, and the fraction of apoptotic ECs presenting with condensed nucleus or apoptotic bodies was calculated. Optical density of immunoglobulin leakage into cerebellar sections was analyzed as follows: digital densitometry was undertaken with a Nikon DS-Fi1 digital camera mounted on a Nikon eclipse E800 microscope and using the Nikon NIS Elements software version 3.10. The autowhite function was applied before each imaging session for white balance. Identical brightness was achieved by using the red-green-blue (RGB) histogram and by setting each of the 3 channels to 225/255 without a slide placed under the objective. Tissue artifacts were strictly avoided. One image per ROI was taken with the 10x objective, resulting in a size of 1.14 $mm^2$. Images were saved as JPEG. To quantify immunoglobulin staining, we used Image J version 1.43r (NIH, MD, USA); the RGB image was split into 8-bit red, green, and blue channels. Next, the blue channel was inverted and the mean density measured.

For histologic analysis, eyes were harvested and fixed 1 hour in 4% glutaraldehyde and then kept in 10% PFA. Eye samples were then embedded in methacrylate. Sections were cut through the pupillary-optic nerve plane and stained with hematoxylin and eosin. Severity of pathologic changes was determined by a scoring system of 0–4 system, as previously detailed.[40]

## Immunohistochemical Evaluation of Samples From Patients With Susac Syndrome

Available biopsy specimens from patients with Susac syndrome were stained with an antiperforin antibody (ab89821, Abcam). In short, sequential 4-μm sections of paraffin-embedded hippocampal specimens were deparaffinized, and antigen retrieval was performed by steaming in Tris buffer (0.01, pH 8.5) with EDTA (0.05 M) for 30 minutes. Primary antibody was applied overnight at 4°C. Incubation with primary antibodies was followed by a biotinylated donkey-antirabbit antibody (711-065-152, Jackson), avidin-peroxidase (016-030-084, Jackson), and DAB development.

Fluorescent triple labeling on these brain samples was performed for perforin, CD8, and CD34. To this end, paraffin-embedded sections were treated as previously described.[39] In short, an antiperforin (ab89821, Abcam) antibody was applied overnight, followed by corresponding biotinylated secondary system and tyramid enhancement. Slides were then steamed in Tris buffer (0.01, pH 8.5) with EDTA (0.05 M) for 30 minutes, followed by 1 hour incubation with Cy2-conjugated streptavidin (016-220-084, Jackson). In a second overnight incubation, anti-CD8 (RM-9116-S0, Neomarkers) and anti-CD34 (NCL-END, Novocastra) primary antibodies were applied together to the tissue, followed by Cy3-conjugated donkey-antirabbit (711-165-152, Jackson) and Cy5-conjugated donkey-antimouse (715-175-151, Jackson) secondary antibodies. Fluorescent preparations were examined using a confocal laser scan microscope (Leica SP5, Leica Mannheim, Germany).

## In Vivo Cytotoxic Function Assay

Splenocytes expressing the CD45.1 marker were incubated for 1 hour at 37°C either with the $HA_{512\text{-}520}$ peptide or a $K^d$-binding control peptide (SYIPSAEKI) and stained with high (1/12,500) or low (1/1,250) dilutions of CTV, respectively. Ten million splenocytes of each population were coinjected in $CD45.2^+$ [BALB/c x C57Bl/6]F1 mice that were transferred with HA-specific CTLs the previous day. Mice were treated with the perforin inhibitor SN34960 or diluent during transfer of splenocytes, and mice were euthanized 12 hours later. The ratio of $CTV^{high}/CTV^{low}$ $CD45.1^+$ B cells was determined by flow cytometry in the spleen of recipient mice, and the percentage of antigen-specific lysis was calculated as follows: [1−(% of B cells pulsed with SYIPSAEKI/% of B cells pulsed with $HA_{512\text{-}520}$) × 100].

## Flow Cytometry

Brain, spleen, and lymph nodes from EC-$HA^+$ and EC-$HA^-$ mice were collected, single-cell suspension was prepared, and nonspecific binding was blocked by an FcR blocking reagent (Miltenyi). Surface staining was performed with directly labeled antibodies (eTable 1, links.lww.com/NXI/A846) in flow cytometry buffer. For intracellular staining, cells were stimulated in vitro with PMA (1 μg/mL, Sigma), ionomycin (1 μg/mL, Sigma), and Golgi Plug (BD) for 4 hours, followed by staining for IFN-γ, TNF, and granzyme B using BD Cytofix/Cytoperm. Data were collected on LSRII Fortessa or Symphony flow cytometers (BD) and analyzed with the FlowJo software (Tree Star).

## Statistics

Statistical analyses were performed using the GraphPad Prism 9.0 software. Data in figures are represented as mean values ± SEM. Statistical significance for normally distributed data was determined using the unpaired, two-tailed Student *t* test or ANOVA tests with post hoc corrections for multiple comparisons. For nonparametric data, the Mann-Whitney test was used. Distribution of qualitative data was compared using the $\chi^2$ test. $p$ Values of less than 0.05 were considered significant and indicated in the corresponding figures (*: $p < 0.05$; **: $p < 0.01$; ***: $p < 0.001$; and ****: $p < 0.0001$).

## Study Approval

Mice were used in accordance with the European Union guidelines following approval of the local ethics committee (2016060714124653V9) and the Research Ministry (APAFIS#29538-2021020121315290).

## Data Availability

Data not provided in the article because of space limitations can be shared at the request of other investigators.

**Figure 1** Coculture of HA-Expressing BBB-ECs With HA-Specific CTLs Leads to an Antigen-Dependent Apoptosis of Endothelial Cells

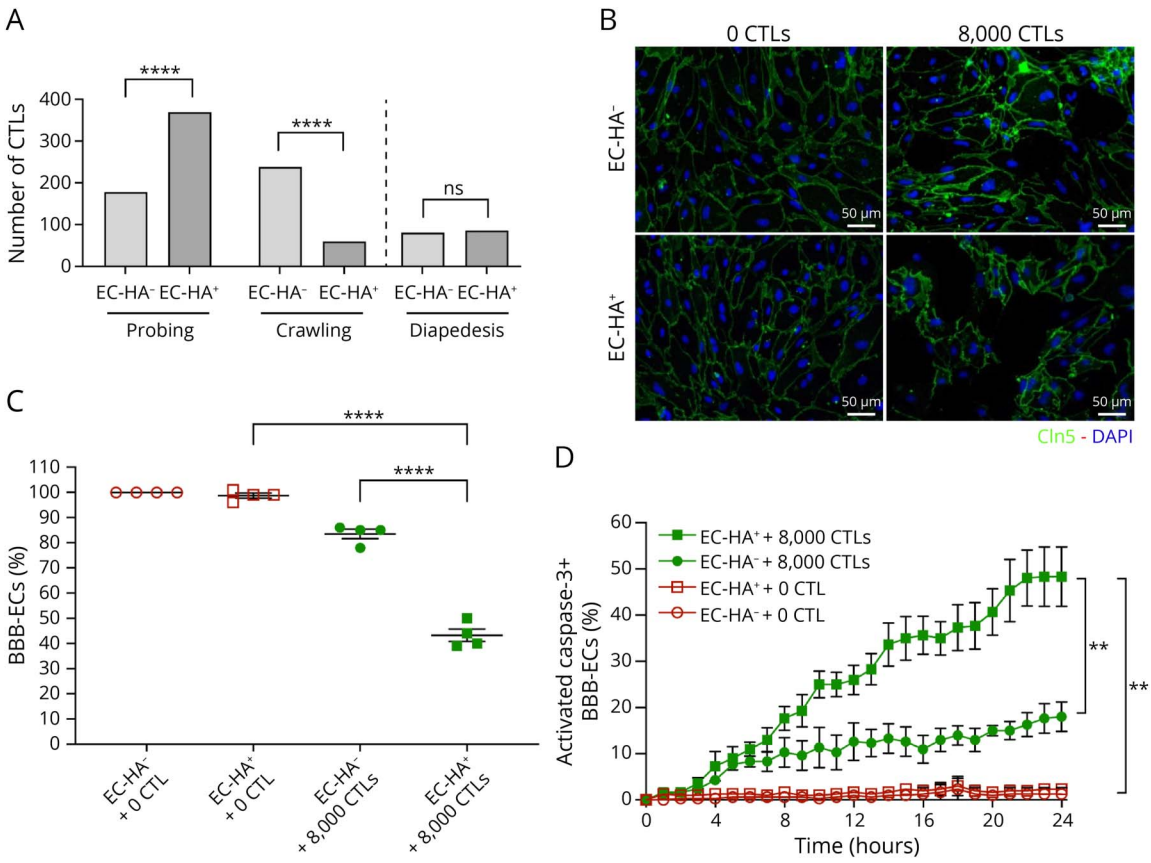


(A) BBB-ECs from EC-HA$^+$ or EC-HA$^-$ mice were superfused for 20 minutes with HA-specific CTLs in a flow chamber. A number of 451 and 444 CTLs were arrested on BBB-ECs from EC-HA$^+$ and EC-HA$^-$ mice, respectively, and then 22 and 28 cells, respectively, detached after their arrest. The fractions of durably arrested CTLs probing and crawling were determined as categorical variables (left) and the fractions undergoing diapedesis (right). Results are from 2 independent experiments. The distribution between groups was compared using the $\chi^2$ test. (B) BBB-ECs from EC-HA$^+$ or EC-HA$^-$ mice were cultured alone or in the presence of 8000 HA-specific CTLs. After 24 hours, BBB-ECs were fixed and stained with DAPI and anticlaudin-5 antibody. (C) DAPI+ nuclei surrounded by claudin-5 staining were counted and, in each experiment, the number of claudin-5–positive ECs in the wells from EC-HA$^-$ mice in the absence of CTLs was used as the 100% reference value. Data from 4 independent experiments are shown as mean and SEM, and the *p* values were determined using one-way ANOVA with post hoc Tukey HSD for multiple comparisons. (D) Kinetic analysis of activated caspase-3 expression in BBB-ECs in culture with or without HA-specific CTLs. Activated caspase-3 activity was determined using a NucView 488 assay and fluorescence microscopy. Data from 3 independent experiments are shown as mean and SEM, and the *p* values were determined using a two-way ANOVA with post hoc Tukey HSD for multiple comparisons. BBB-EC = endothelial cells of the blood-brain barrier; CTLs = cytotoxic CD8 T cells; EC = endothelial cells; HA = hemagglutinin.

# Results

## Recognition of Cognate Antigen Presented by Brain Endothelial Cells Modifies CTL Mobility

We developed an in vitro system to investigate the mechanisms and consequences of antigen-specific interactions between highly purified primary mouse BBB-ECs, expressing HA or not, and HA-specific transgenic CTLs. The BBB-ECs grew as an adherent cell monolayer in vitro and expressed homogeneously claudin-5, a prototypic marker of ECs from the BBB (eFigure 1A, links.lww.com/NXI/A837). The HA-specific CTLs expressed high levels of IFN-γ, TNF, FasL, CD107a, granzyme B, and perforin (eFigure 1B).

We first monitored the behavior of the HA-specific CTLs after their initial interaction with BBB-ECs using live in vitro cell imaging under physiologic flow conditions.[36,41] On addition over BBB-ECs, the HA-specific CTLs became arrested on the brain ECs at a similar rate, regardless of their HA expression. On evaluation of the postarrest behavior, HA-specific CTLs adopted a predominant crawling behavior on the BBB-ECs from EC-HA$^-$ mice, whereas they stalled on the BBB-ECs from EC-HA$^+$ mice and exhibited a probing behavior (Figure 1A). During the period of investigation (20 minutes), HA expression by the BBB-ECs did not result in enhanced transmigration of the CTLs (Figure 1A) or EC damage. Thus, changes in CD8 T-cell mobility behavior were induced on antigen recognition on BBB-ECs over a short observation period.

## CTLs Induce Antigen-Dependent Apoptosis of Brain Endothelial Cells

To study the interactions of HA-expressing or control BBB-EC monolayers with HA-specific CTLs over a longer timeframe, a coculture system without flow was implemented. Antigen-specific loss of ECs was induced by the CTLs after 24 hours,

**Figure 2** Antigen-Dependent Apoptosis of BBB-ECs Is Inhibited by a Perforin Inhibitor

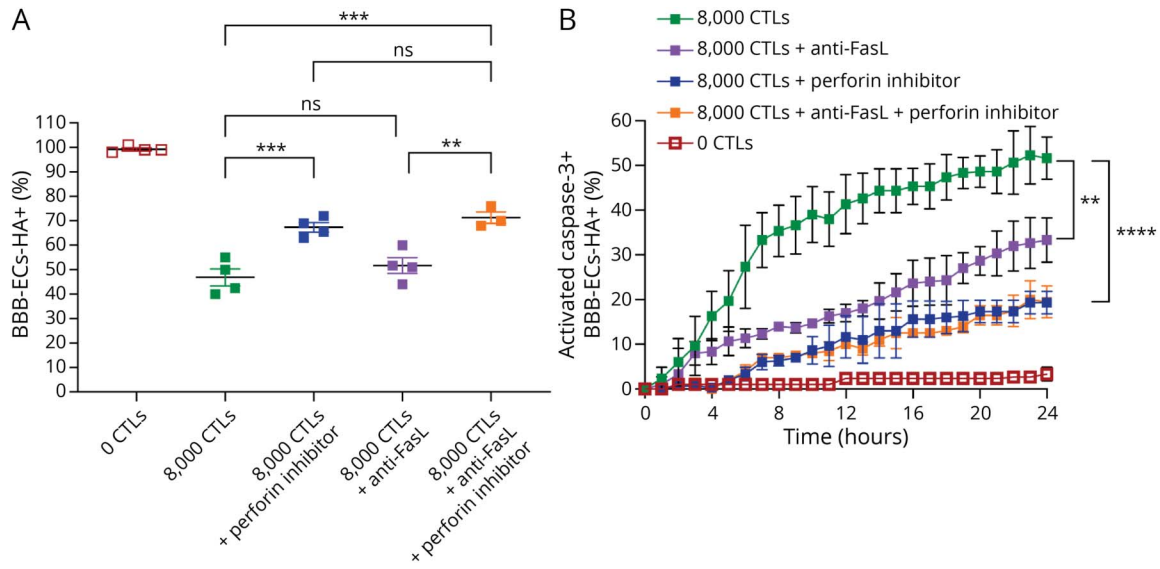


BBB-ECs from EC-HA$^+$ mice were cultured alone or in the presence of 8000 HA-specific CTLs, in the presence or absence of a perforin inhibitor and/or a neutralizing anti-FasL mAb. (A) After 24 hours, BBB-ECs were fixed and stained with DAPI and claudin-5. Numbers of BBB-ECs nuclei after the 24 hours coculture are shown. The 100% value was set from the number of nuclei in the culture of BBB-ECs from EC-HA$^-$ mice without CTLs (see eFigure 2, links.lww.com/NXI/A838). Data represent the mean and SEM of 3–4 independent experiments, and the *p* values were determined using one-way ANOVA, followed by Sidak correction for multiple comparisons. (B) Kinetics of caspase-3 activation in BBB-ECs from EC-HA$^+$ mice during the coculture with or without perforin inhibitor and/or anti-FasL mAb. Activated caspase-3 activity was determined using a NucView 488 assay and fluorescence microscopy. Data represent the mean and SEM of 3–4 independent experiments, and the *p* values were determined using two-way ANOVA with post hoc Tukey HSD for multiple comparisons. BBB-EC = endothelial cells of the blood-brain barrier; CTLs = cytotoxic CD8 T cells; EC = endothelial cells; HA = hemagglutinin.

with a 56.7% decrease in the number of HA-expressing BBB-ECs compared with a 16.5% reduction of control BBB-ECs (Figure 1, B and C). To determine whether the specificity of the CTLs was important for the death of HA-expressing BBB-ECs, we compared the effect of HA-specific CTLs and ovalbumin-specific OT-I CTLs in the same coculture system. Only HA-specific CTLs were able to preferentially induce loss of HA-expressing BBB-ECs (eFigure 2A, links.lww.com/NXI/A838).

To assess the mechanism of loss of HA-expressing BBB-ECs on their interaction with CTLs, we used a fluorescent apoptosis detection assay based on caspase 3 activation. The HA-expressing and control BBB-EC monolayers were imaged longitudinally, in the presence or absence of HA-specific CTLs. In the absence of CTLs, little if any expression of active caspase-3 was observed in the 2 BBB-EC cultures (Figure 1D). On addition of HA-specific CTLs, the proportion of BBB-ECs from EC-HA$^+$ mice expressing active caspase-3 progressively increased to reach 48.3% after 24 hours, but remained significantly smaller (18%) in control BBB-ECs (Figure 1D). These data collectively demonstrate that CTLs promoted a rapid and marked loss of BBB-ECs through apoptotic death in an antigen-specific manner.

## Pharmacologic Inhibition of Perforin Decreases Antigen-Specific Apoptosis of HA-Expressing Brain Endothelial Cells In Vitro

We next explored the molecular pathways involved in the antigen-specific killing of BBB-ECs from EC-HA$^+$ mice by HA-specific CTLs. The high expression of proapoptotic molecules such as granzyme B and FasL, together with the surface expression of lysosomal marker CD107a by HA-specific CTLs, suggested that target cell death might be triggered through the granule-dependent pathway and/or through ligation of Fas on the target cells (eFigure 1B, links.lww.com/NXI/A837). To distinguish these possibilities, the cocultures of HA-expressing BBB-ECs and CTLs were conducted in the presence of a blocking anti-FasL mAb and/or a perforin inhibitor (a small molecule benzenesulfonamide derivative designated SN34960), which prevents the coalescence of perforin monomers into transmembrane pores,[37] thereby preventing the delivery of apoptosis-triggering granzymes into the target cell cytosol. Consistent with the experiments described earlier (Figure 1C), 54.2% of HA-expressing BBB-ECs became detached and were lost after 24 hours when perforin and FasL were not inhibited (Figure 2A). However, the loss of ECs was reduced to 33.2% in the presence of the perforin inhibitor, whereas the anti-FasL mAb did not significantly inhibit antigen-specific killing. The combined use of both inhibitors provided no added protection of the BBB-ECs above that afforded by the perforin inhibitor alone (Figure 2A). Monitoring of caspase 3-dependent apoptosis for 24 hours revealed that the perforin inhibitor very significantly inhibited the antigen-dependent activation of caspase-3 in HA-expressing BBB-ECs (Figure 2B) from the fifth hour onward. The anti-FasL mAb provided a significant, but less marked, decrease in caspase-3 activation, but this did not translate into reduced destruction of BBB-ECs. Once again,

**Figure 3** Treatment With the Perforin Inhibitor Alleviates the Clinical Signs and Decreases Damage of the BBB in a Preclinical Model of Neuroinflammatory Disease

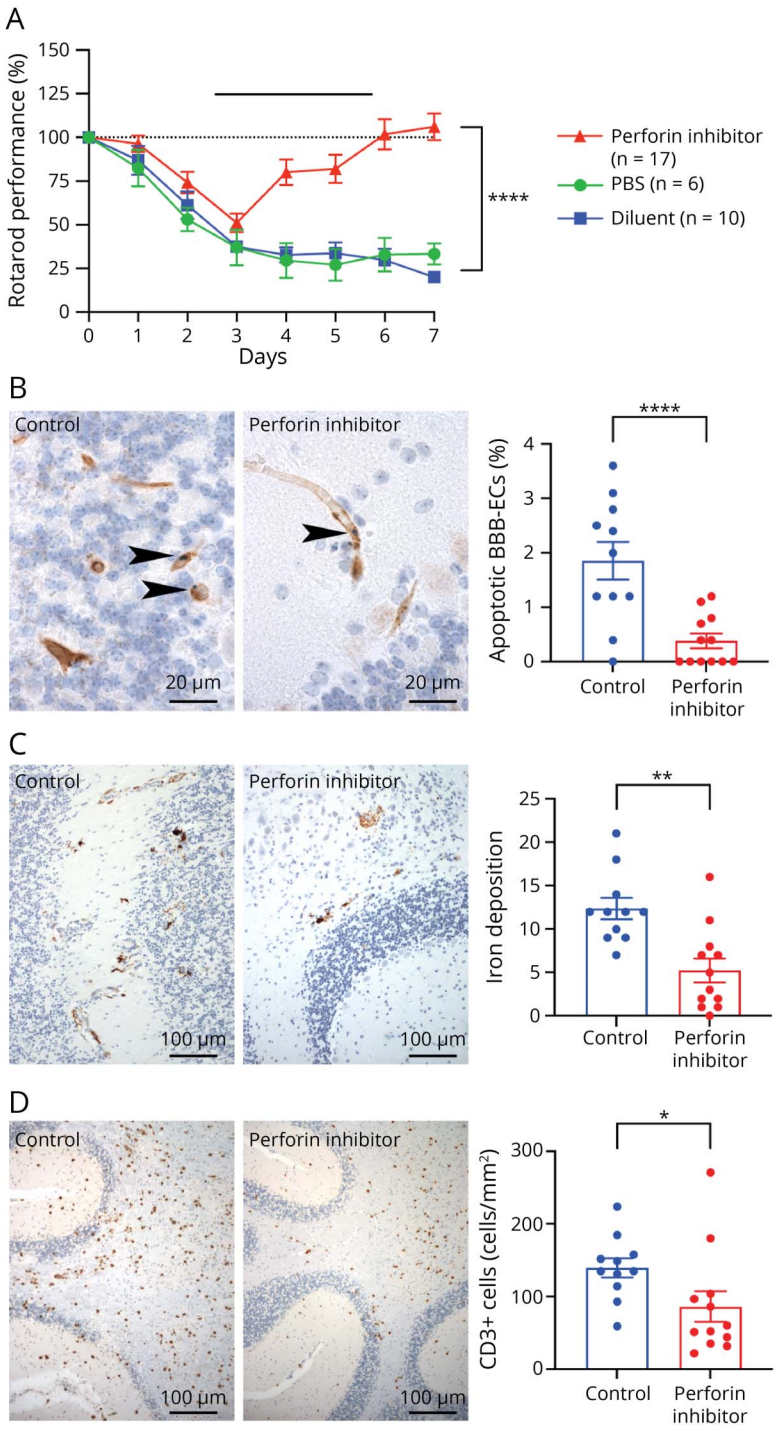


(A) Motor performance assessed by Rotarod in EC-HA$^+$ mice after adoptive transfer of HA-specific CTLs. Mice were treated with PBS, diluent or perforin inhibitor every 12 hours, from day 3 until sacrifice at day 7 post-CTL transfer. The 100% was set from the motor performance at day 0, before CTL transfer. Bar shows the treatment period. Data are pooled from 3 independent experiments. Two-way ANOVA was used to determine the *p* values. (B–D) Frequency of apoptotic BBB-ECs (B), iron deposition (C), and infiltration of CD3$^+$ T cells (D) in the brain of CTL-injected EC-HA$^+$ mice, treated or not with the perforin inhibitor. The control EC-HA$^+$ mice received either diluent or PBS. Data represent the mean and SEM of 11–12 mice per group from 3 independent experiments, and the *p* values were determined using the Student *t* test. BBB = blood-brain barrier; BBB-EC = endothelial cells of the blood-brain barrier; EC = endothelial cells; HA = hemagglutinin.

the combination of anti-FasL mAb and perforin inhibitor did not further reduce caspase-3 activation in BBB-ECs. Of note, neither the perforin inhibitor nor the anti-FasL mAb had a significant impact on the minor antigen-independent killing of BBB-ECs from EC-HA$^-$ mice by the HA-specific CTLs (eFigure 3, links.lww.com/NXI/A839).

Collectively, the data indicate that perforin plays a nonredundant role in the antigen-specific killing of BBB-ECs by CTLs in vitro. Conversely, the FasL/Fas pathway is dispensable because the resultant level of procaspase-3 processing through this mechanism did not reach a lethal threshold.

**Figure 4** Treatment With the Perforin Inhibitor Reduces Infiltration of the CNS by Immune Cells in a Preclinical Model of Neuroinflammatory Disease

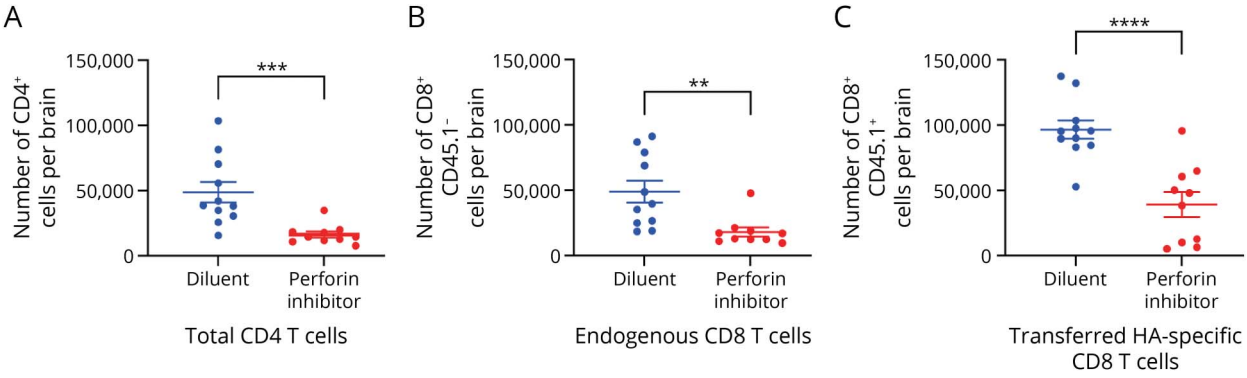


(A) Number of CD4, (B) endogenous, and (C) transferred CD8 T cells infiltrating the CNS of EC-HA$^+$ mice, 7 days after adoptive transfer of CTLs and 4 days after initiation of treatment. Data represent the mean and SEM of 3 independent experiments. For panels A and B, the *p* values were determined using the Mann-Whitney test, and for panel C, the *p* values were determined using the Student *t* test.

## Treatment With Perforin Inhibitor SN34960 Enables Swift Recovery of Motor Functions in a Preclinical Model of Neuroinflammatory Disease

Based on these in vitro data, we next tested whether in vivo administration of the perforin inhibitor SN34960 could inhibit the development and progression of a CD8 T cell–mediated inflammatory disease of the CNS. First, we showed that the perforin inhibitor had no impact on motor performance by itself (eFigure 4A, links.lww.com/NXI/A840). We next demonstrated that SN34960 could inhibit killing of HA-presenting target cells in vivo using a quantitative cytotoxicity assay. To this end, splenocytes loaded with HA peptide or control peptide were cotransferred (1:1 ratio) into recipient mice hosting various numbers of HA-specific CTLs. The perforin inhibitor reproducibly reduced destruction of HA peptide-loaded target cells in vivo, and the level of protection was greater (approximately 60% vs 25%) when fewer CTLs were infused ($3 \times 10^5$ vs $1 \times 10^6$) (eFigure 4B–C, links.lww.com/NXI/A839).

As a first step toward clinical development, we next tested the therapeutic impact of pharmacologic perforin inhibition in a preclinical model of neuroinflammatory disease that mimics SuS. As recently published,[14] the adoptive transfer of HA-specific CTLs into EC-HA$^+$ mice induced a CD8 T cell–mediated endotheliopathy restricted to the retina and CNS, which resulted in motor dysfunction from day 2 onward (Figure 3A). To further investigate the antigen specificity of our in vivo model, we injected EC-HA$^+$ mice with either HA-specific CTLs or ovalbumin-specific OT-I CTLs. Only EC-HA$^+$ recipient mice injected with HA-specific CTLs exhibited clinical signs (eFigure 2B, links.lww.com/NXI/A838) and prominent infiltration of transferred CTLs in the brain (eFigure 2C). Perforin was detected in the CNS of diseased mice, particularly in the lumen of brain microvessels (eFigure 4D, links.lww.com/NXI/A840). Of interest, in postmortem samples from patients with Sus, we identified perforin-expressing CD8 T cells in contact with brain microvessel ECs, suggesting that a cytotoxic mechanism involving perforin might be at play (eFigure 5, links.lww.com/NXI/A841).

Mice were treated for 4 days with the perforin inhibitor SN34960 starting at day 3 after disease induction, when the neurologic signs were already established. The administration of the perforin inhibitor resulted in clear improvement in motor performances within 24 hours and complete recovery after 3 days of treatment (Figure 3A). Immunohistochemistry of brains from EC-HA$^+$ mice revealed a decreased frequency of apoptotic BBB-ECs in mice treated with the perforin inhibitor (Figure 3B). This EC protection was associated with fewer perivascular microhemorrhages, as assessed by Turnbull blue staining (Figure 3C). The CNS parenchyma of EC-HA$^+$ mice treated with SN34960 also exhibited a significant decrease of infiltrating CD3$^+$ T cells (Figure 3D). Furthermore, a significant correlation between immunoglobulin leakage into the CNS parenchyma and BBB-ECs apoptosis (eFigure 6A, links.lww.com/NXI/A842) or T-cell infiltration (eFigure 6B) was noted. The perforin inhibitor also significantly decreased the extent of retinal lesions (eFigure 6C).

To further identify the immunologic correlates of the therapeutic efficacy of perforin inhibition, the immune cell infiltration in the CNS was analyzed in greater depth using flow cytometry. Seven days after CTL injection, T-cell infiltration was present in all EC-HA$^+$ mice, whether treated with the perforin inhibitor or not. However, mice that received the perforin inhibitor exhibited significantly fewer transferred (CD45.1$^+$) HA-specific CTLs and fewer endogenous CD4 and CD8 T cells infiltrating their brain parenchyma (Figure 4, A–C and eFigure 7A, links.lww.com/NXI/A843). Despite the reduction in HA-specific CD8 T cells infiltrating the CNS in the perforin

**Figure 5** Perforin Inhibitor Allows Quicker and Stable Recovery Despite Treatment Discontinuation

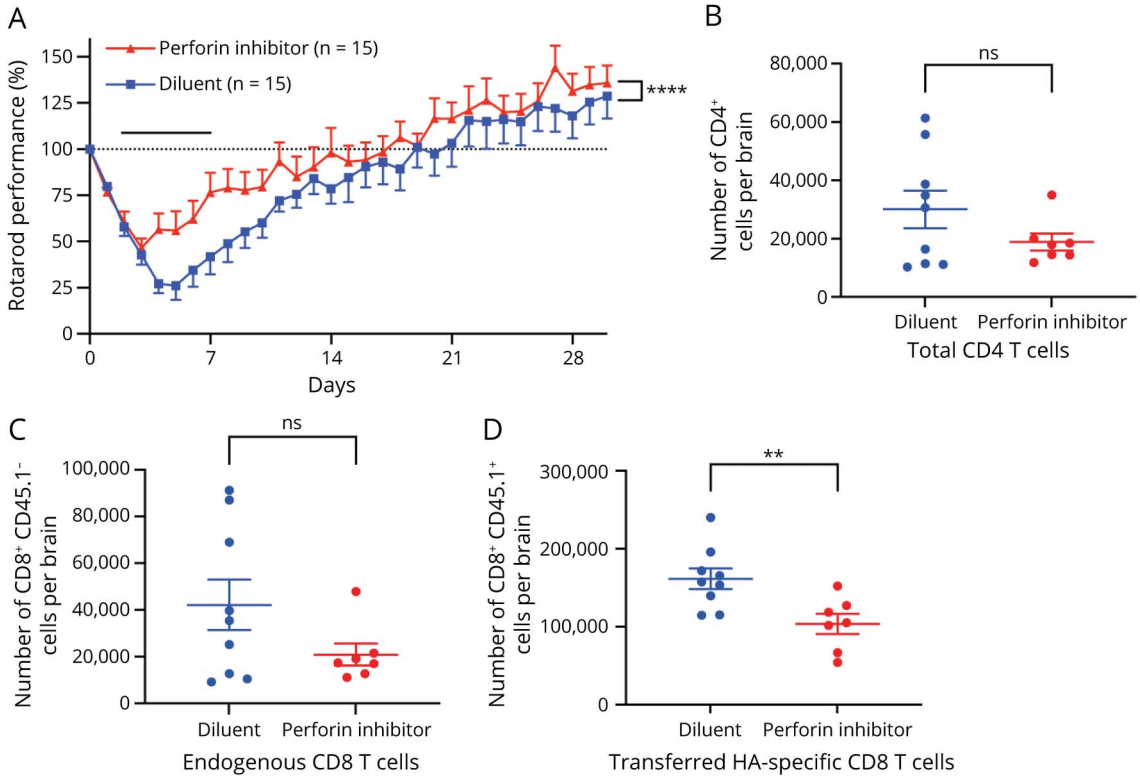


(A) Motor performance assessed by Rotarod in EC-HA$^+$ mice after adoptive transfer of HA-specific CTLs. Mice were treated with diluent or perforin inhibitor from day 3 to day 7 after CTL transfer and sacrificed at day 30. The 100% was set from the motor performance at day 0, before CTL transfer. Bar shows the treatment period. Data are pooled from 4 independent experiments. Two-way ANOVA was used to determine the *p* values. (B) Number of CD4, (C) endogenous, and (D) transferred CD8 T cells infiltrating the CNS of EC-HA$^+$ mice, 30 days after adoptive transfer of CTLs. Data represent the mean and SEM of 2 independent experiments. The *p* values were determined using the Mann-Whitney test for panels B and C and the Student *t* test for panel D.

inhibitor–treated EC-HA$^+$ mice (Figure 4C), no significant difference was noted in the number of infiltrating blood-derived myeloid cells or in the activation status of microglial cells (eFigure 7, B and C). We then interrogated the phenotypic and functional status of CNS-infiltrating HA-specific CD8 T cells from EC-HA$^+$ mice treated or not with the perforin inhibitor. We identified no notable phenotypic differences between HA-specific CD8 T cells from perforin inhibitor–treated and untreated EC-HA$^+$ mice (eFigure 8, links.lww.com/NXI/A844). Thus, the perforin inhibitor seemed to affect the CNS-infiltrating T cells quantitatively rather than qualitatively.

In contrast to the CNS findings, no decrease was noted in the number of transferred HA-specific CTLs present in the spleen, cervical lymph nodes, and CNS distant (inguinal) lymph nodes of treated EC-HA$^+$ recipient mice, indicating that pharmacologic perforin inhibition impaired the CNS transmigration of T cells rather than reducing their overall survival (eFigure 9, A and B, links.lww.com/NXI/A845). Of note, a sizeable fraction of peripheral HA-specific CD8 T cells exhibited an activated phenotype (eFigure 9, C–E). Notably, this activated phenotype was more marked in the cervical lymph nodes, particularly after perforin inhibitor therapy, possibly reflecting their recent activation by the BBB-ECs (eFigure 9E).

Given this heightened activation phenotype exhibited by the HA-specific CTLs, we evaluated whether transient (4 days) perforin inhibition would induce sustained clinical benefit or whether the disease manifestations would rebound after treatment cessation. New cohorts of EC-HA$^+$ mice were therefore followed up for 3 weeks after treatment withdrawal. In line with our earlier results, treatment with the perforin inhibitor enabled rapid recovery when compared with sham-treated EC-HA$^+$ mice and, importantly, the motor benefit was sustained (Figure 5A). Moreover, the number of CNS-infiltrating cells at day 30 was decreased in both groups when compared with those at day 7 (Figures 4 and 5), but little differences between treatment groups were noted for the numbers of endogenous CD4 and CD8 T cells and myeloid cell populations (Figure 5, B and C and eFigure 7, D and E, links.lww.com/NXI/A843). Nevertheless, EC-HA$^+$ mice treated with the perforin inhibitor showed a sustained decrease in the number of CNS-infiltrating transferred HA-specific CTLs (Figure 5D). Overall, our study reveals the sustained benefit of transient in vivo inhibition of the perforin pathway in a preclinical model of CD8 T cell–mediated

neuroinflammation based on clinical, immunologic, and histopathologic outcomes.

## Discussion

We report that perforin-dependent cytotoxicity is a key mediator of the death of BBB-ECs that present a neo self-antigen in an MHC class I–restricted manner to antigen-specific effector CD8 T cells. This antigen-specific interaction led to changes in CD8 T-cell mobility in vitro, with an increased probing of the BBB-ECs, culminating in overt BBB-EC apoptosis, which we observed both in vitro and in vivo. Critically, our studies showed that short-term pharmacologic inhibition of perforin, the apical regulator of the granule exocytosis pathway, largely reversed the CD8 T cell–mediated neurologic impairment that followed BBB-EC disruption. The therapeutic mechanism of action involved a marked reduction of BBB-EC apoptosis and, consequently, of T-cell infiltration into the CNS.

Circulating CD8 T cells recognizing CNS self-antigens are present not only in patients with neurodegenerative and neuroinflammatory diseases but also in healthy individuals.[42] In principle, CD8 T cells could migrate to the CNS through 1 or more of the barriers separating the CNS from the periphery, namely through the leptomeninges, the choroid plexus, and the BBB.[16,43,44] The role of BBB-ECs has attracted much attention because they can promote Ag-independent and Ag-specific interactions with effector CD8 T cells. Indeed, BBB-ECs express MHC class I molecules in experimental models[45,46] and in humans[47] and can also express costimulatory molecules.[20,24,48]

The distinctive advantage of our model is to directly investigate the antigen-specific interactions between effector CD8 T cells and BBB-ECs. We showed that this interaction led to marked antigen-specific loss of BBB-ECs through apoptotic cell death. This is reminiscent of the role described for ECs in other organs, where they contribute to the T-cell infiltration and immunopathogenesis.[26,49,50] In experimental cerebral malaria (ECM), parasite-specific CD8 T cells are arrested on both the luminal and abluminal surfaces of the venous cerebrovascular system after recognition of parasitic antigens cross-presented by the ECs, resulting in BBB breakdown associated with BBB-EC death.[46,51] Likewise, significant numbers of granzyme-producing effector CD8 T cells were identified in contact with BBB-ECs in children with fatal cerebral malaria,[52] associated with a significantly increased proportion of not only ECs but also neurons and glial cells, exhibiting apoptotic features.[53]

Different molecular pathways account for CD8 T cell–mediated apoptosis, but gene knock-out studies in mice and a variety of human immunodeficiencies have shown that they do not contribute equally to target cell death. First, the release of TNF family members and IFN-$\gamma$ by CD8 T cells can induce an indirect apoptosis through stimulation of macrophages or a direct effect leading to an apoptotic cascade in the target cells.[54] Second, engagement of Fas by FasL expressed on CD8 T cells initiates the activation of apical procaspase-8 or 10 through the formation of a death-inducing signaling complex at the inner leaflet of the target cell membrane.[55] Third, perforin released into the immune synapse by exocytosis of CTLs' secretory granules forms pores in the membrane of the target cell membrane that allow serine protease granzymes released from the same cytotoxic granules to diffuse into the target cell cytosol[56] to activate apoptosis.[57] This pathway accounts for most of the cytotoxic activity of CD8 T cells, as shown by the marked susceptibility of perforin-null mice to viral infections.[58]

Because a perforin inhibitor showed promising results in a model of EC apoptosis in fulminant viral hepatitis,[26] we assessed its effectiveness in our model of CD8 T cell–mediated neuroinflammation. In doing so, we were aware that ECs may have variable characteristics depending on their organ of origin.[24] The perforin inhibitor SN34960 binds specifically to perforin monomers released into the immune synapse, thereby preventing the assembly of perforin pores that typically comprise 24 monomers.[38,59] It has been shown that the compound SN34960 does not cause the death of CTLs if they are incubated for several days in medium containing the inhibitor. T-cell proliferation, progression through the cell cycle, and T-cell activation remain normal.[60] In vitro, our results showed that perforin plays a major role in the antigen-specific killing of BBB-ECs by CTLs, whereas the Fas pathway seemed dispensable. This is in accordance with results in cerebral malaria where polarization of granzyme B toward brain ECs was noted.[53] We then assessed the effects of short-term perforin inhibition in our preclinical model, when the disease was already established and signs were peaking. Despite the induction of a severe disease in control mice, we observed a rapid and total reversal of neurologic signs by the perforin inhibitor, as early as 24 hours after treatment initiation. The improved motor performance and the reduced antigen-specific T-cell infiltration persisted long after treatment discontinuation. Because our model, induced by a single injection of CTLs, is monophasic, it would be necessary to test this perforin inhibitor in a model involving chronic targeting of the BBB-ECs to evaluate more precisely its longer-term effects.

Of importance, we found that the perforin inhibitor had no effect on the systemic CD8 T-cell compartment, attesting its selectivity. The short duration of the treatment and its focus only on activated CD8 T cells makes it unlikely that deleterious effects such as systemic cytokine hypersecretion, which has been observed in children born with a total and congenital absence of perforin function, will be encountered.[61]

To conclude, we describe in this study that BBB-ECs and CTLs are capable of antigen-specific interactions resulting in BBB-ECs apoptosis mainly involving the perforin/granzyme pathway. In the preclinical model, both the clinical manifestations and underlying immunopathology were effectively inhibited by short-term pharmacologic intervention with a

perforin inhibitor. Therefore, perforin represents a potential therapeutic target for SuS and other CD8 T cell–mediated neuroinflammatory diseases.


## Acknowledgment

The authors are indebted to the Cytometry and Imaging platforms of Infinity and to T. Vermeulen for her technical help. The authors thank the UMS06 for mouse care and histological platform and Drs A. Saoudi and D. Dunia for their critical reading of the manuscript.

## Study Funding

This work was supported by grants from Agence Nationale pour la Recherche CE17-0014 (RSL), Fondation pour la Recherche Médicale (Prix Line Pomaret Delalande [CGF]; DEQ20170336727 [RSL]) ARSEP-French MS society: ARSEP 2019-20 (RSL), BETPSY RHU 18- RHUS-0012 (RSL), Austrian Science Fund FWF: P34864-B (JB). The early stages of perforin inhibitor drug development were funded by the Strategic Drug Discovery Initiative (SDDI) Program of the Wellcome Trust UK (JAT).


## Disclosure

C. Fonte, E. Dufourd, V. Cazaentre, S. Aydin, B. Engelhardt, R. R. Caspi, B. Xu, G. Martin-Blondel, J.A. Spicer, and C. Bost report no disclosures relevant to the manuscript. C. Gonzalez-Fierro reports financial support by Fondation pour la Recherche Médicale (FRM). R.S. Liblau reports financial support by Fondation pour la Recherche Médicale (FRM), the French MS society (ARSEP foundation), Agence Nationale pour la Recherche CE17-0014, and BETPSY RHU 18- RHUS-0012. J. Bauer reports financial support by Austrian Science Fund FWF: P34864-B. J.A. Trapani reports financial support by the Strategic Drug Discovery Initiative (SDDI) Program of the Wellcome Trust UK. Go to Neurology.org/NN for full disclosure.


## Publication History

Received by *Neurology: Neuroimmunology & Neuroinflammation* August 1, 2022. Accepted in final form February 21, 2023. Submitted and externally peer reviewed. The handling editor was Editor Josep O. Dalmau, MD, PhD, FAAN.


## Appendix Authors

| Name | Location | Contribution |
|---|---|---|
| **Carmen Gonzalez-Fierro, MSc** | Toulouse Institute for infectious and inflammatory diseases (Infinity), University of Toulouse, CNRS, INSERM, UPS, France | Drafting/revision of the article for content, including medical writing for content; major role in the acquisition of data; study concept or design; and analysis or interpretation of data |
| **Coralie Fonte, PhD** | Toulouse Institute for infectious and inflammatory diseases (Infinity), University of Toulouse, CNRS, INSERM, UPS, France | Major role in the acquisition of data |
| **Eloïse Dufourd, MSc** | Toulouse Institute for infectious and inflammatory diseases (Infinity), University of Toulouse, CNRS, INSERM, UPS, France | Major role in the acquisition of data |
| **Vincent Cazaentre, BSc** | Toulouse Institute for infectious and inflammatory diseases (Infinity), University of Toulouse, CNRS, INSERM, UPS, France | Major role in the acquisition of data |
| **Sidar Aydin, PhD** | Theodor Kocher Institute, University of Bern, Switzerland | Major role in the acquisition of data |
| **Britta Engelhardt, PhD** | Theodor Kocher Institute, University of Bern, Switzerland | Drafting/revision of the article for content, including medical writing for content |
| **Rachel R. Caspi, PhD** | Laboratory of Immunology, National Eye Institute, National Institutes of Health, Bethesda, MD | Drafting/revision of the article for content, including medical writing for content |
| **Biying Xu, PhD** | Laboratory of Immunology, National Eye Institute, National Institutes of Health, Bethesda, MD | Major role in the acquisition of data |
| **Guillaume Martin-Blondel, MD, PhD** | Toulouse Institute for infectious and inflammatory diseases (Infinity), University of Toulouse, CNRS, INSERM, UPS; Department of Infectious and Tropical diseases, Toulouse University Hospital, France | Drafting/revision of the article for content, including medical writing for content; study concept or design |
| **Julie A. Spicer, PhD** | Auckland Cancer Society Research Centre, Faculty of Medical and Health Sciences, The University of Auckland, New Zealand | Provided the perforin inhibitor SN34960 |
| **Joseph A. Trapani, MD, PhD** | Cancer Immunology Program, Peter MacCallum Cancer Centre, Melbourne; Sir Peter MacCallum Department of Oncology, The University of Melbourne, Parkville, Australia | Drafting/revision of the article for content, including medical writing for content; additional contributions: provided the perforin inhibitor SN34960 |
| **Jan Bauer, PhD** | Department of Neuroimmunology, Center for Brain Research, Medical University of Vienna, Austria | Drafting/revision of the article for content, including medical writing for content; major role in the acquisition of data |
| **Roland S. Liblau, MD, PhD** | Toulouse Institute for infectious and inflammatory diseases (Infinity), University of Toulouse, CNRS, INSERM, UPS; Department of Immunology, Toulouse University Hospital, France | Drafting/revision of the article for content, including medical writing for content; study concept or design; and analysis or interpretation of data |
| **Chloé Bost, PharmD, PhD** | Toulouse Institute for infectious and inflammatory diseases (Infinity), University of Toulouse, CNRS, INSERM, UPS; Department of Immunology, Toulouse University Hospital, France | Drafting/revision of the article for content, including medical writing for content; study concept or design |

## References


1. Waisman A, Liblau RS, Becher B. Innate and adaptive immune responses in the CNS. *Lancet Neurol.* 2015;14(9):945-955. doi:10.1016/s1474-4422(15)00141-6
2. McCandless EE, Zhang B, Diamond MS, Klein RS. CXCR4 antagonism increases T cell trafficking in the central nervous system and improves survival from West Nile virus encephalitis. *Proc Natl Acad Sci U S A.* 2008;105(32):11270-11275. doi:10.1073/pnas.0800898105
3. Frieser D, Pignata A, Khajavi L, et al. Tissue-resident CD8+ T cells drive compartmentalized and chronic autoimmune damage against CNS neurons. *Sci Transl Med.* 2022;14(640):eabl6157. doi:10.1126/scitranslmed.abl6157
4. Vincenti I, Page N, Steinbach K, et al. Tissue-resident memory CD8+ T cells cooperate with CD4+ T cells to drive compartmentalized immunopathology in the CNS. *Sci Transl Med.* 2022;14(640):eabl6058. doi:10.1126/scitranslmed.abl6058
5. Zhang D, Ren J, Luo Y, et al. T cell response in ischemic stroke: from mechanisms to translational insights. *Front Immunol.* 2021;12:707972. doi:10.3389/fimmu.2021.707972
6. Gate D, Saligrama N, Leventhal O, et al. Clonally expanded CD8 T cells patrol the cerebrospinal fluid in Alzheimer's disease. *Nature.* 2020;577(7790):399-404. doi:10.1038/s41586-019-1895-7
7. Galiano-Landeira J, Torra A, Vila M, Bové J. CD8 T cell nigral infiltration precedes synucleinopathy in early stages of Parkinson's disease. *Brain.* 2020;143(12):3717-3733. doi:10.1093/brain/awaa269
8. Machado-Santos J, Saji E, Tröscher AR, et al. The compartmentalized inflammatory response in the multiple sclerosis brain is composed of tissue-resident CD8+ T lymphocytes and B cells. *Brain.* 2018;141(7):2066-2082. doi:10.1093/brain/awy151
9. Babbe H, Roers A, Waisman A, et al. Clonal expansions of CD8+ T cells dominate the T cell infiltrate in active multiple sclerosis lesions as shown by micromanipulation and single cell polymerase chain reaction. *J Exp Med.* 2000;192(3):393-404. doi:10.1084/jem.192.3.393
10. Beltrán E, Gerdes LA, Hansen J, et al. Early adaptive immune activation detected in monozygotic twins with prodromal multiple sclerosis. *J Clin Invest.* 2019;129(11):4758-4768. doi:10.1172/jci128475
11. Bien CG, Vincent A, Barnett MH, et al. Immunopathology of autoantibody-associated encephalitides: clues for pathogenesis. *Brain.* 2012;135(5):1622-1638. doi:10.1093/brain/aws082
12. Pignolet BSL, Gebauer CMT, Liblau RS. Immunopathogenesis of paraneoplastic neurological syndromes associated with anti-Hu antibodies: a beneficial antitumor immune response going awry. *Oncoimmunology.* 2013;2(12):e27384. doi:10.4161/onci.27384
13. Yshii L, Bost C, Liblau R. Immunological bases of paraneoplastic cerebellar degeneration and therapeutic implications. *Front Immunol.* 2020;11:991. doi:10.3389/fimmu.2020.00991
14. Gross CC, Meyer C, Bhatia U, et al. CD8+ T cell-mediated endotheliopathy is a targetable mechanism of neuro-inflammation in Susac syndrome. *Nat Commun.* 2019;10(1):5779. doi:10.1038/s41467-019-13593-5
15. Scalise AA, Kakogiannos N, Zanardi F, Iannelli F, Giannotta M. The blood–brain and gut–vascular barriers: from the perspective of claudins. *Tissue Barriers.* 2021;9(3):1926190. doi:10.1080/21688370.2021.1926190
16. Marchetti L, Engelhardt B. Immune cell trafficking across the blood-brain barrier in the absence and presence of neuroinflammation. *Vasc Biol.* 2020;2(1):H1–H18. doi:10.1530/vb-19-0033
17. Kawakami N, Nägerl UV, Odoardi F, Bonhoeffer T, Wekerle H, Flügel A. Live imaging of effector cell trafficking and autoantigen recognition within the unfolding autoimmune encephalomyelitis lesion. *J Exp Med.* 2005;201(11):1805-1814. doi:10.1084/jem.20050011
18. Bartholomäus I, Kawakami N, Odoardi F, et al. Effector T cell interactions with meningeal vascular structures in nascent autoimmune CNS lesions. *Nature.* 2009;462(7269):94-98. doi:10.1038/nature08478
19. Howland SW, Claser C, Poh CM, Gun SY, Rénia L. Pathogenic CD8+ T cells in experimental cerebral malaria. *Semin Immunopathol.* 2015;37(3):221-231. doi:10.1007/s00281-015-0476-6
20. Wheway J, Obeid S, Couraud PO, Combes V, Grau GER. The brain microvascular endothelium supports T cell proliferation and has potential for alloantigen presentation. *PLoS One.* 2013;8(1):e52586-e52588. doi:10.1371/journal.pone.0052586
21. Liebner S, Dijkhuizen RM, Reiss Y, Plate KH, Agalliu D, Constantin G. Functional morphology of the blood–brain barrier in health and disease. *Acta Neuropathol.* 2018;135(3):311-336. doi:10.1007/s00401-018-1815-1
22. Daneman R. The blood-brain barrier in health and disease. *Ann Neurol.* 2012;72(5):648-672. doi:10.1002/ana.23648
23. Munji RN, Soung AL, Weiner GA, et al. Profiling the mouse brain endothelial transcriptome in health and disease models reveals a core blood-brain barrier dysfunction module. *Nat Neurosci.* 2019;22(11):1892-1902. doi:10.1038/s41593-019-0497-x
24. Kalucka J, de Rooij LP, Goveia J, et al. Single-cell transcriptome atlas of murine endothelial cells. *Cell.* 2020;180(4):764-779.e20. doi:10.1016/j.cell.2020.01.015
25. Galea I, Bernardes-Silva M, Forse PA, van Rooijen N, Liblau RS, Perry VH. An antigen-specific pathway for CD8 T cells across the blood-brain barrier. *J Exp Med.* 2007;204(9):2023-2030. doi:10.1084/jem.20070064
26. Welz M, Eickhoff S, Abdullah Z, et al. Perforin inhibition protects from lethal endothelial damage during fulminant viral hepatitis. *Nat Commun* 2018;9(1):4805. doi:10.1038/s41467-018-07213-x
27. Rudd-Schmidt JA, Trapani JA, Voskoboinik I. Distinguishing perforin-mediated lysis and granzyme-dependent apoptosis. *Methods Enzymol.* 2019;629:291-306. doi:10.1016/bs.mie.2019.07.034
28. Marrodan M, Fiol MP, Correale J. Susac syndrome: challenges in the diagnosis and treatment. *Brain.* 2022;145(3):858-871. doi:10.1093/brain/awab476
29. Hay ZLZ, Slansky JE. Granzymes: the molecular executors of immune-mediated cytotoxicity. *Int J Mol Sci.* 2022;23(3):1833. doi:10.3390/ijms23031833
30. Voskoboinik I, Whisstock JC, Trapani JA. Perforin and granzymes: function, dysfunction and human pathology. *Nat Rev Immunol.* 2015;15(6):388-400. doi:10.1038/nri3839
31. Saxena A, Bauer J, Scheikl T, et al. Cutting edge: multiple sclerosis-like lesions induced by effector CD8 T cells recognizing a sequestered antigen on oligodendrocytes. *J Immunol.* 2008;181(3):1617-1621. doi:10.4049/jimmunol.181.3.1617
32. Ridder DA, Lang MF, Salinin S, et al. TAK1 in brain endothelial cells mediates fever and lethargy. *J Exp Med.* 2011;208(13):2615-2623. doi:10.1084/jem.20110398
33. Hogquist KA, Jameson SC, Heath WR, Howard JL, Bevan MJ, Carbone FR. T cell receptor antagonist peptides induce positive selection. *Cell.* 1994;76(1):17-27. doi:10.1016/0092-8674(94)90169-4
34. Coisne C, Dehouck L, Faveeuw C, et al. Mouse syngenic in vitro blood-brain barrier model: a new tool to examine inflammatory events in cerebral endothelium. *Lab Invest.* 2005;85(6):734-746. doi:10.1038/labinvest.3700281
35. Steiner O, Coisne C, Cecchelli R, et al. Differential roles for endothelial ICAM-1, ICAM-2, and VCAM-1 in shear-resistant T cell arrest, polarization, and directed crawling on blood–brain barrier endothelium. *J Immunol.* 2010;185(8):4846-4855. doi:10.4049/jimmunol.0903732
36. Abadier M, Haghayegh Jahromi N, Cardoso Alves L, et al. Cell surface levels of endothelial ICAM-1 influence the transcellular or paracellular T-cell diapedesis across the blood-brain barrier. *Eur J Immunol.* 2015;45(4):1043-1058. doi:10.1002/eji.201445125
37. Spicer JA, Miller CK, O'Connor PD, et al. Benzenesulphonamide inhibitors of the cytolytic protein perforin. *Bioorg Med Chem Lett.* 2017;27(4):1050-1054. doi:10.1016/j.bmcl.2016.12.057
38. Spicer JA, Huttunen KM, Jose J, et al. Small molecule inhibitors of lymphocyte perforin as focused immunosuppressants for infection and autoimmunity. *J Med Chem.* 2022;65(21):14305-14325. doi:10.1021/acs.jmedchem.2c01338
39. Bauer J, Lassmann H. Neuropathological techniques to investigate central nervous system sections in multiple sclerosis. *Methods Mol Biol.* 2016;1304:211-229. doi:10.1007/7651_2014_151
40. Chan CC, Caspi RR, Ni M, et al. Pathology of experimental autoimmune uveoretinitis in mice. *J Autoimmun.* 1990;3(3):247-255. doi:10.1016/0896-8411(90)90144-h
41. Rudolph H, Klopstein A, Gruber I, Blatti C, Lyck R, Engelhardt B. Postarrest stalling rather than crawling favors CD8+ over CD4+ T-cell migration across the blood–brain barrier under flow in vitro. *Eur J Immunol.* 2016;46(9):2187-2203. doi:10.1002/eji.201546251
42. Sulzer D, Alcalay RN, Garretti F, et al. T cells from patients with Parkinson's disease recognize α-synuclein peptides. *Nature.* 2017;546(7660):656-661. doi:10.1038/nature22815
43. Louveau A, Herz J, Alme MN, et al. CNS lymphatic drainage and neuroinflammation are regulated by meningeal lymphatic vasculature. *Nat Neurosci.* 2018;21(10):1380-1391. doi:10.1038/s41593-018-0227-9
44. Strazielle N, Creidy R, Malcus C, Boucraut J, Ghersi-Egea JF. T-lymphocytes traffic into the brain across the blood-CSF barrier: evidence using a reconstituted choroid plexus epithelium. *PLoS One.* 2016;11(3):e0150945. doi:10.1371/journal.pone.0150945
45. Yang YM, Shang DS, Zhao WD, Fang WG, Chen YH. Microglial TNF-α-dependent elevation of MHC class I expression on brain endothelium induced by amyloid-beta promotes T cell transendothelial migration. *Neurochem Res.* 2013;38(11):2295-2304. doi:10.1007/s11064-013-1138-5
46. Howland SW, Poh CM, Rénia L. Activated brain endothelial cells cross-present malaria antigen. *PLoS Pathog.* 2015;11(6):e1004963. doi:10.1371/journal.ppat.1004963
47. Zang YCQ, Li S, Rivera VM, et al. Increased CD8 + cytotoxic T cell responses to myelin basic protein in multiple sclerosis. *J Immunol.* 2004;172(8):5120-5127. doi:10.4049/jimmunol.172.8.5120
48. Lopes Pinheiro MA, Kamermans A, Garcia-Vallejo JJ, et al. Internalization and presentation of myelin antigens by the brain endothelium guides antigen-specific T cell migration. *Elife.* 2016;5(6):e13149. doi:10.7554/elife.13149
49. Bracamonte-Baran W, Gilotra NA, Won T, et al. Endothelial stromal PD-L1 (programmed death ligand 1) modulates CD8 + T-cell infiltration after heart transplantation. *Circ Heart Fail.* 2021;14(10):e007982. doi:10.1161/circheartfailure.120.007982
50. Bender C, Rajendran S, von Herrath MG. New insights into the role of autoreactive CD8 T cells and cytokines in human type 1 diabetes. *Front Endocrinol (Lausanne).* 2021;11:606434. doi:10.3389/fendo.2020.606434
51. Swanson PA, Hart GT, Russo MV, et al. CD8+T cells induce fatal brainstem pathology during cerebral malaria via luminal antigen-specific engagement of brain vasculature. *PLoS Pathog.* 2016;12(12):e1006022. doi:10.1371/journal.ppat.1006022
52. Riggle BA, Manglani M, Maric D, et al. CD8+ T cells target cerebrovasculature in children with cerebral malaria. *J Clin Invest.* 2020;130(3):1128-1138. doi:10.1172/jci133474
53. Punsawad C, Maneerat Y, Chaisri U, Nantavisai K, Viriyavejakul P. Nuclear factor kappa B modulates apoptosis in the brain endothelial cells and intravascular leukocytes of fatal cerebral malaria. *Malar J.* 2013;12(1):260. doi:10.1186/1475-2875-12-260
54. Brincks EL, Katewa A, Kucaba TA, Griffith TS, Legge KL. CD8 T cells utilize TRAIL to control influenza virus infection. *J Immunol.* 2008;181(10):4918-4925. doi:10.4049/jimmunol.181.7.4918
55. Chávez-Galán L, Arenas-Del Angel MC, Zenteno E, Chávez R, Lascurain R. Cell death mechanisms induced by cytotoxic lymphocytes. *Cell Mol Immunol.* 2009;6(1):15-25. doi:10.1038/cmi.2009.3

56. Lopez JA, Susanto O, Jenkins MR, et al. Perforin forms transient pores on the target cell plasma membrane to facilitate rapid access of granzymes during killer cell attack. *Blood*. 2013;121(14):2659-2668. doi:10.1182/blood-2012-07-446146
57. Sutton VR, Wowk ME, Cancilla M, Trapani JA. Caspase activation by granzyme B is indirect, and caspase autoprocessing requires the release of proapoptotic mitochondrial factors. *Immunity*. 2003;18(3):319-329. doi:10.1016/s1074-7613(03)00050-5
58. Kägi D, Ledermann B, Bürki K, et al. Cytotoxicity mediated by T cells and natural killer cells is greatly impaired in perforin-deficient mice. *Nature*. 1994;369(6475):31-37. doi:10.1038/369031a0
59. Ivanova ME, Lukoyanova N, Malhotra S, et al. The pore conformation of lymphocyte perforin. *Sci Adv* 2022;8(6):eabk3147. doi:10.1126/sciadv.abk3147
60. Gartlan KH, Jaiswal JK, Bull MR, et al. Preclinical activity and pharmacokinetic/pharmacodynamic relationship for a series of novel benzenesulfonamide perforin inhibitors. *ACS Pharmacol Transl Sci* 2022;5(6):429-439. doi:10.1021/acsptsci.2c00009
61. Stepp SE, Dufourcq-Lagelouse R, Deist FL, et al. Perforin gene defects in familial hemophagocytic lymphohistiocytosis. *Science* 1999;286(5446):1957-1959. doi:10.1126/science.286.5446.1957

# Effects of a Small-Molecule Perforin Inhibitor in a Mouse Model of CD8 T Cell–Mediated Neuroinflammation

Carmen Gonzalez-Fierro, Coralie Fonte, Eloïse Dufourd, et al.

*Neurol Neuroimmunol Neuroinflamm* 2023;10;
DOI 10.1212/NXI.0000000000200117